  Bull. Chem. Soc. Jpn., 55, 1063—1072 (1982) 

# Structural Study of Optical Resolution. XI. The Crystal Structures of $(+)_{589}$-Tris(biguanide)cobalt(III) Chloride *d*-Tartrate Trihydrate and Racemic Tris(biguanide)cobalt(III) Trichloride

Toshiji TADA, Yoshihiko KUSHI, and Hayami YONEDA*

*Department of Chemistry, Faculty of Science, Hiroshima University, Higashi-senda-machi, Naka-ku, Hiroshima 730*

(Received September 9, 1981)

The crystal structures of the more-soluble diastereomeric salt, $(+)_{589}$-$[Co(Hbg)_3]Cl(d\text{-tart})\cdot 3H_2O$ (**1**), and the racemic chloride salt, $[Co(Hbg)_3]Cl_3$ (**2**), have been determined by X-ray analysis ($R=0.033$, 2788 reflections for **1** and $R=0.056$, 2785 reflections for **2**), where $Hbg=C_2H_7N_5$, $d\text{-tart}=C_4H_4O_6^{2-}$. The more-soluble salt **1** is orthorhombic, with the space group $P2_12_12_1$, $Z=4$, $a=15.654(2)$, $b=13.758(2)$, and $c=11.010(1)$ Å. The racemic salt **2** is monoclinic, with the space group C2/c, $Z=8$, $a=19.441(9)$, $b=14.901(7)$, $c=15.911(6)$ Å, and $\beta=127.63(2)°$. In **1**, the complex cations and the $Cl^-$ ions are arranged alternately to form an infinite spiral chain, $\{\Delta\text{-}[Co(Hbg)_3]Cl\}_\infty$. Each *d*-tartrate is hydrogen-bonded to a twofold-screw-axis-related neighbor (-OH··· OOC- 2.792 Å) to form an infinite chain, $(d\text{-tart})_\infty$. In **2** two kinds of similar infinite spiral chains, $\{\Delta\text{-}[Co(Hbg)_3]Cl\}_\infty$ and $\{\Lambda\text{-}[Co(Hbg)_3]Cl\}_\infty$, which are mirror images of each other are found. The structures of these two salts **1** and **2** are compared with those of the less-soluble diastereomeric chloride *d*-tartrate and the optically active chloride in both of which a similar infinite chain has been found, and the mechanism of chiral discrimination *via* the diastereomer formation is discussed.

In a previous paper, we reported the crystal structure of the less-soluble diastereomeric salt, $(-)_{589}$-$[Co(Hbg)_3]Cl(d\text{-tart})\cdot 5H_2O$ **3** (Hbg stands for biguanide, and *d*-tart stands for the *d*-tartrate ion).[1] Two characteristic features were noted to be important in connection with the mechanism of optical resolution *via* the less-soluble diastereomeric salt: 1) The chiral complex and $Cl^-$ ions are arranged alternately to form an infinite spiral chain which is cationic and left-handed as a whole, and 2) two *d*-tart anions exist closely to each other and form a dimeric unit with 4 negative charges, similar in structure to the antimony *d*-tartrate ion. Such a dimeric unit of *d*-tart anions has never been found in the crystal structures determined so far. A similar infinite spiral chain was found in the optically active chloride salt, $(+)_{589}$-$[Co(Hbg)_3]Cl_3\cdot H_2O$.[2] In this case, the spiral chain consists of $\Delta$ complexes and is right-handed as a whole. With these findings in mind, we have attempted here to determine the crystal structures of the more-soluble diastereomeric salt, $(+)_{589}$-$[Co(Hbg)_3]Cl(d\text{-tart})\cdot 3H_2O$ **1**, as well as the racemic chloride salt, $[Co(Hbg)_3]Cl_3$ **2**, in order to see whether the infinite spiral chain of the complex ions exists in common and to see how the *d*-tart anions are packed in the more-soluble salt **1**. Through these crystal structure analyses, we have tried to find out a clue to the mechanism of optical resolution of the biguanide complex.

## Experimental

*Preparation of Compound.* Biguanide sulfate was prepared by the method given in the literature.[3] The racemic chloride salt, $[Co(Hbg)_3]Cl_3$ **2**, was prepared by the method of Ray and Dutt.[4] The crystals are brownish yellow parallelepiped. Found: C, 15.60; H, 4.56; N, 45.10%. Calcd for $CoC_6H_{21}N_{15}Cl_3$: C, 15.38; H, 4.52; N, 44.83%. The more-soluble diastereomeric salt, $(+)_{589}$-$[Co(Hbg)_3]Cl(d\text{-tart})\cdot 3H_2O$ **1**, was prepared by the method of Ray and Dutt.[5] After removal of the crystals of the less-soluble diastereomeric salt **3**, the filtrate was allowed to stand at room temperature for several days. Large and thick plate-like crystals of the more-soluble salt were easily separated mechanically from the fine thin plates of the remaining less-soluble salt. The optical purity of the crystals was checked by the CD measurement ($\Delta\varepsilon_{510}=+3.52$ and $\Delta\varepsilon_{452}=-4.76$).[6] Found: C, 19.37; H, 4.96; N, 35.90%. Calcd for $CoC_{10}H_{25}N_{15}O_6Cl\cdot 3H_2O$ ($2H_2O$): C, 20.02 (20.64); H, 5.21 (5.02); N, 35.03 (36.11)%.

*Data Collection.* The size of crystal used for the X-ray measurement was 0.53 mm × 0.32 mm × 0.15 mm for the more-soluble salt **1** and 0.25 mm × 0.13 mm × 0.08 mm for the racemic salt **2**. For **1**, the systematic absences for *h*00 ($h=2n+1$), 0*k*0 ($k=2n+1$), and 00*l* ($l=2n+1$) indicated the space group $P2_12_12_1$. For **2**, the systematic absences for *hkl* ($h+k=2n+1$) and *h*0*l* ($h=2n+1$ and $l=2n+1$) suggested the following possible space groups: Cc and C2/c. The three-dimensional Patterson map indicated the space group C2/c and the success of the structure determination confirmed the wisdom of this selection. The determination of cell dimensions and the collection of intensity data were carried out on a Rigaku AFC-5 automated four-circle diffractometer with Mo $K\alpha$ radiation ($\lambda=0.71069$ Å) monochromated by a graphite plate. Both unit-cell dimensions were refined by a least-squares method with 23 high angle reflections ($2\theta>26°$). The crystal data are summarized in Table 1. Densities of the

Table 1. Crystallographic data

| | *a*/Å | *b*/Å | *c*/Å | *β*/° | Space group | *Z* | $D_m$/g cm$^{-3}$ | $D_c$/g cm$^{-3}$ | *V*/Å$^3$ | (*V*/*Z*)/Å$^3$ |
|---|---|---|---|---|---|---|---|---|---|---|
| (1) | 15.654(2) | 13.758(2) | 11.010(1) | — | $P2_12_12_1$ | 4 | $1.66_3$ | 1.680 | 2371.2(5) | 592.8(1) |
| (2) | 19.441(9) | 14.901(7) | 15.911(6) | 127.63(2) | C2/c | 8 | $1.67_5$ | 1.705 | 3635(3) | 456.3(3) |
| (3) | 24.846(5) | 12.970(2) | 8.645(2) | — | C222 | 4 | $1.51_4$ | 1.516 | 2785.8(8) | 696.5(2) |
| (4) | 18.675(9) | 14.086(7) | 15.004(7) | — | $C222_1$ | 8 | 1.64(2) | 1.637 | 3947(5) | 493.4(6) |

(1): $(+)_{589}$-$[Co(Hbg)_3]Cl(d\text{-tart})\cdot 3H_2O$. (2): $[Co(Hbg)_3]Cl_3$. (3): $(-)_{589}$-$[Co(Hbg)_3]Cl(d\text{-tart})\cdot 5H_2O$.[1] (4): $(+)_{589}$-$[Co(Hbg)_3]Cl_3\cdot H_2O$ reported by Snow.[2]

TABLE 2. POSITIONAL AND THERMAL PARAMETERS FOR $(+)_{589}$-$[Co(Hbg)_3]Cl(d\text{-tart})\cdot 3H_2O$

| Atom | $x$ | $y$ | $z$ | $B_{eq}$/Å$^{2}$ a) |
|---|---|---|---|---|
| Co | 0.75979(3) | 0.60488(3) | 0.48673(4) | 2.20 |
| Cl | 0.99932(7) | 0.52598(9) | 0.20659(12) | 4.42 |
| N(A1) | 0.8344(2) | 0.5131(2) | 0.4089(3) | 2.82 |
| N(A2) | 0.9003(2) | 0.3653(3) | 0.3680(4) | 3.95 |
| N(A3) | 0.7738(2) | 0.3687(2) | 0.4755(3) | 3.37 |
| N(A4) | 0.6549(2) | 0.3391(2) | 0.5902(3) | 3.58 |
| N(A5) | 0.6923(2) | 0.4981(2) | 0.5464(3) | 2.78 |
| N(B1) | 0.8277(2) | 0.7079(2) | 0.4226(3) | 2.63 |
| N(B2) | 0.8538(3) | 0.8525(3) | 0.3179(4) | 4.49 |
| N(B3) | 0.7256(2) | 0.7744(2) | 0.2932(3) | 3.09 |
| N(B4) | 0.6082(2) | 0.7043(3) | 0.2052(4) | 3.39 |
| N(B5) | 0.6878(2) | 0.6150(2) | 0.3447(3) | 2.85 |
| N(C1) | 0.8315(2) | 0.6056(2) | 0.6282(3) | 2.64 |
| N(C2) | 0.9061(2) | 0.6837(3) | 0.7818(3) | 4.02 |
| N(C3) | 0.7831(2) | 0.7528(2) | 0.7089(3) | 2.97 |
| N(C4) | 0.6505(2) | 0.8223(2) | 0.6947(4) | 3.87 |
| N(C5) | 0.6852(2) | 0.6933(2) | 0.5673(3) | 2.48 |
| C(A1) | 0.8354(2) | 0.4199(3) | 0.4163(3) | 2.75 |
| C(A2) | 0.7046(2) | 0.4063(3) | 0.5375(3) | 2.66 |
| C(B1) | 0.8045(2) | 0.7744(3) | 0.3484(3) | 2.78 |
| C(B2) | 0.6739(2) | 0.6935(3) | 0.2834(3) | 2.74 |
| C(C1) | 0.8409(2) | 0.6771(3) | 0.7024(3) | 2.58 |
| C(C2) | 0.7047(2) | 0.7542(3) | 0.6533(3) | 2.54 |
| CT1 | 0.7490(2) | 0.9070(2) | 1.0193(3) | 3.16 |
| CT2 | 0.8069(3) | 0.9674(3) | 0.9368(3) | 2.90 |
| CT3 | 0.8997(3) | 0.9562(3) | 0.9764(4) | 3.39 |
| CT4 | 0.9589(3) | 1.0097(3) | 0.8880(5) | 4.55 |
| OT1 | 0.7121(2) | 0.8344(2) | 0.9740(3) | 4.27 |
| OT2 | 0.7434(2) | 0.9334(2) | 1.1275(3) | 4.63 |
| OT3 | 0.7973(2) | 0.9370(2) | 0.8139(3) | 3.78 |
| OT4 | 0.9189(2) | 0.8541(2) | 0.9802(3) | 4.11 |
| OT5 | 1.0204(2) | 0.9662(3) | 0.8452(5) | 6.47 |
| OT6 | 0.9421(3) | 1.0952(3) | 0.8649(5) | 7.66 |
| OW1 | 0.5067(2) | 0.7450(3) | 0.4974(5) | 6.17 |
| OW2 | 0.9677(5) | 0.9341(4) | 0.5893(5) | 11.00 |
| OW3 | 0.5431(3) | 0.8421(5) | 0.0183(6) | 11.74 |
| H(NA1) | 0.878(2) | 0.537(3) | 0.359(4) | 1.90 |
| H(NA21) | 0.882(4) | 0.312(5) | 0.352(6) | 5.91 |
| H(NA22) | 0.937(3) | 0.359(3) | 0.304(4) | 2.70 |
| H(NA3) | 0.784(3) | 0.311(4) | 0.472(5) | 4.26 |
| H(NA41) | 0.661(3) | 0.282(3) | 0.573(4) | 2.15 |
| H(NA42) | 0.609(4) | 0.362(4) | 0.622(5) | 4.44 |
| H(NA5) | 0.649(3) | 0.513(4) | 0.585(5) | 3.54 |
| H(NB1) | 0.880(4) | 0.709(4) | 0.442(6) | 4.62 |
| H(NB21) | 0.839(4) | 0.885(4) | 0.253(5) | 4.24 |
| H(NB22) | 0.901(3) | 0.861(4) | 0.356(5) | 3.63 |
| H(NB3) | 0.713(3) | 0.830(3) | 0.253(4) | 2.14 |
| H(NB41) | 0.578(3) | 0.650(4) | 0.185(5) | 3.13 |
| H(NB42) | 0.607(4) | 0.746(4) | 0.163(6) | 4.49 |
| H(NB5) | 0.658(3) | 0.556(3) | 0.318(4) | 1.92 |
| H(NC1) | 0.868(3) | 0.553(3) | 0.645(4) | 1.55 |
| H(NC21) | 0.950(4) | 0.643(4) | 0.769(5) | 5.17 |
| H(NC22) | 0.906(3) | 0.722(3) | 0.835(4) | 2.30 |
| H(NC3) | 0.798(3) | 0.806(3) | 0.756(4) | 1.18 |
| H(NC41) | 0.671(4) | 0.864(4) | 0.738(5) | 4.48 |
| H(NC42) | 0.599(5) | 0.879(6) | 0.654(8) | 10.52 |
| H(NC5) | 0.626(3) | 0.693(3) | 0.541(5) | 2.69 |
| H(CT2) | 0.788(3) | 1.033(3) | 0.948(4) | 1.65 |

Table 2. (Continued)

| Atom | $x$ | $y$ | $z$ | $B_{eq}$/Å$^{2}$ a) |
|---|---|---|---|---|
| H(CT3) | 0.910(3) | 0.986(3) | 1.057(4) | 1.91 |
| H(OT3) | 0.792(3) | 0.987(3) | 0.763(4) | 2.54 |
| H(OT4) | 0.966(4) | 0.838(4) | 0.982(5) | 4.79 |
| H(OW11) | 0.538(4) | 0.784(4) | 0.451(6) | 5.81 |
| H(OW12) | 0.497(3) | 0.686(4) | 0.468(5) | 4.13 |
| H(OW21) | 0.984(4) | 1.007(4) | 0.581(7) | 6.48 |
| H(OW22) | 0.932(4) | 0.892(5) | 0.668(6) | 6.52 |
| H(OW31) | 0.616(4) | 0.849(5) | 0.003(6) | 6.37 |
| H(OW32) | 0.483(5) | 0.769(6) | 0.017(10) | 11.71 |

a) $B_{eq}=8\pi^2(U_{11}+U_{22}+U_{33})/3$.

Table 3. Positional and thermal parameters for $[Co(Hbg)_3]Cl_3$

| Atom | $x$ | $y$ | $z$ | $B_{eq}$/Å$^{2}$ a) |
|---|---|---|---|---|
| Co | 0.18928(5) | 0.12498(5) | 0.25003(6) | 1.68 |
| Cl(1) | 0.3650(1) | 0.3747(1) | 0.4800(1) | 3.09 |
| Cl(2) | 0.4575(1) | 0.0066(1) | 0.6026(1) | 3.30 |
| Cl(3) | 0.3950(1) | 0.7434(1) | 0.6027(1) | 3.12 |
| N(A1) | 0.2213(3) | 0.0615(3) | 0.1745(4) | 2.44 |
| N(A2) | 0.3131(4) | 0.0041(4) | 0.1408(6) | 4.50 |
| N(A3) | 0.3557(4) | 0.1253(5) | 0.2499(7) | 5.97 |
| N(A4) | 0.4217(4) | 0.2469(4) | 0.3594(6) | 4.25 |
| N(A5) | 0.2969(3) | 0.1888(4) | 0.3259(4) | 2.37 |
| N(B1) | 0.0817(3) | 0.0632(3) | 0.1726(4) | 2.13 |
| N(B2) | −0.0168(4) | −0.0528(4) | 0.1223(5) | 3.56 |
| N(B3) | 0.1249(3) | −0.0692(3) | 0.2699(5) | 2.71 |
| N(B4) | 0.2532(4) | −0.1104(4) | 0.4236(5) | 3.51 |
| N(B5) | 0.2406(3) | 0.0315(3) | 0.3545(4) | 2.09 |
| N(C1) | 0.1358(3) | 0.2188(3) | 0.1454(4) | 2.37 |
| N(C2) | 0.0796(5) | 0.3615(4) | 0.0767(5) | 4.43 |
| N(C3) | 0.1053(4) | 0.3193(4) | 0.2303(5) | 4.09 |
| N(C4) | 0.1121(5) | 0.3028(5) | 0.3792(6) | 5.92 |
| N(C5) | 0.1595(3) | 0.1875(3) | 0.3287(4) | 2.31 |
| C(A1) | 0.2928(4) | 0.0628(4) | 0.1871(5) | 3.20 |
| C(A2) | 0.3566(4) | 0.1879(4) | 0.3135(5) | 2.57 |
| C(B1) | 0.0622(4) | −0.0159(4) | 0.1856(5) | 2.68 |
| C(B2) | 0.2089(4) | −0.0453(4) | 0.3510(5) | 2.57 |
| C(C1) | 0.1076(4) | 0.2954(4) | 0.1489(5) | 2.35 |
| C(C2) | 0.1259(4) | 0.2659(4) | 0.3130(5) | 2.88 |
| H(NA1) | 0.186(4) | 0.010(5) | 0.135(5) | 1.78 |
| H(NA21) | 0.368(5) | 0.012(6) | 0.153(7) | 3.56 |
| H(NA22) | 0.274(5) | −0.030(5) | 0.103(6) | 2.76 |
| H(NA3) | 0.400(7) | 0.119(8) | 0.258(8) | 5.50 |
| H(NA41) | 0.466(5) | 0.237(5) | 0.366(6) | 1.83 |
| H(NA42) | 0.426(7) | 0.295(7) | 0.402(9) | 6.36 |
| H(NA5) | 0.298(5) | 0.236(6) | 0.367(7) | 3.55 |
| H(NB1) | 0.039(5) | 0.094(5) | 0.127(6) | 1.70 |
| H(NB21) | −0.053(5) | −0.024(5) | 0.069(6) | 2.59 |
| H(NB22) | −0.027(6) | −0.115(6) | 0.133(7) | 4.01 |
| H(NB3) | 0.114(6) | −0.123(7) | 0.274(7) | 4.30 |
| H(NB41) | 0.233(5) | −0.160(6) | 0.422(7) | 3.27 |
| H(NB42) | 0.306(5) | −0.094(6) | 0.471(7) | 3.15 |
| H(NB5) | 0.301(5) | 0.048(5) | 0.412(6) | 2.88 |
| H(NC1) | 0.136(4) | 0.207(5) | 0.091(6) | 1.50 |
| H(NC21) | 0.063(8) | 0.409(8) | 0.089(9) | 7.17 |
| H(NC22) | 0.077(6) | 0.367(6) | 0.026(7) | 4.33 |
| H(NC3) | 0.084(5) | 0.374(6) | 0.227(6) | 3.10 |
| H(NC41) | 0.132(5) | 0.277(5) | 0.440(6) | 2.46 |
| H(NC42) | 0.080(5) | 0.360(6) | 0.362(6) | 3.04 |
| H(NC5) | 0.169(5) | 0.159(6) | 0.380(6) | 2.75 |

a) $B_{eq}=8\pi^2(U_{11}+U_{22}+U_{33})/3$.

crystals were measured by the flotation method in a mixture of chloroform and bromoform. The intensity data were collected in the $\omega$-$2\theta$ scan mode up to $2\theta=55°$ with scan rates of 6°/min for **1** and of 16°/min for **2** (50 kV, 170 mA). The $\omega$ scan range was $(1.0+0.5\tan\theta)°$. Of the 2949 and 3322 unique observed reflections, 2788 and 2785 reflections with $|Fo|\geq 3\sigma(F)$ were used for the structure determination in **1** and **2** respectively. Corrections for the absorption effect were neglected ($\mu$(Mo $K\alpha$)=8.96 cm$^{-1}$ for **1** and 14.42 cm$^{-1}$ for **2**).

## Determination and Refinement of Crystal Structures

*The More-soluble Diastereomeric Salt, $(+)_{589}$-[Co(Hbg)$_3$]Cl(*d*-tart). $3H_2O$ (**1**).* The structure was determined by the heavy-atom method and refined by the block-diagonal least-squares method. Three kinds of water molecules were found on a difference Fourier map after the other non-hydrogen atoms were located by an application of the Fourier method. The refinement using anisotropic thermal parameters for non-hydrogen atoms reduced the $R$ value (defined as $\sum||F_o|-|F_c||/\sum|F_o|$) to 0.061. At this stage, all the hydrogen atoms were located from a difference Fourier map. The final refinement including the contribution of these H atoms with isotropic temperature factors converged the $R$ value to 0.033. The final difference map showed no peaks higher than 0.4 electron/Å$^3$. The absolute configuration of $(+)_{589}$-$[Co(Hbg)_3]^{3+}$ was assigned as $\Delta$ on the basis of the configuration (2*R*, 3*R*) of the *d*-tart anion as an internal reference.[7]

*The Racemic Chloride Salt, [Co(Hbg)$_3$]Cl$_3$ (**2**).* The determination and the refinement of the structure were made in a way similar to that used for **1**. The final refinement converged the $R$ value to 0.058. The final difference map showed no peaks higher than 0.4 electron/Å$^3$.

In the refinement, the quantity minimized was $\sum w(|F_o|-k|F_c|)^2$. The weighting scheme used was $w=(\sigma_{CS}^2+a|F_o|+(b|F_o|)^2)^{-1}$, where $\sigma_{CS}$ is the standard deviation obtained from the counting statistics for each reflection; the values of $a$ and $b$ were 0.2 and 0.03 respectively. All the atomic scattering factors, with the effect of the anomalous dispersion of Co and Cl atoms were taken from the International Tables for X-Ray Crystallography, Vol. IV.[8]

All the computations were carried out by a HITAC M-180 computer at the Hiroshima University Information Processing Center. The computer programs used were FOUR-MMM, FOUR-2/M,[9] and HBLS-IV with a slight modification.[10] An ORTEP drawing was carried out by a computer system, XTL, in a Syntex R3 automated four-circle diffractometer.[11] The final atomic parameters are listed in Table 2 for the more-soluble salt **1** and in Table 3 for the racemic salt **2**, respectively. The anisotropic thermal parameters and complete lists of the $|F_o|$ and $|F_c|$ values have been preserved by the Chemical Society of Japan (Document No. 8220).

## Results and Discussion

The projections of the crystal structure for the more-soluble diastereomeric salt **1**, $(+)_{589}$-[Co(Hbg)$_3$]Cl(*d*-tart)·3H$_2$O, along the a- and c-axes are shown in Figs. 1 and 2. The projections of the crystal structure for the racemic chloride salt **2**, [Co(Hbg)$_3$]Cl$_3$, to the (110) plane and along the b-axis are shown in Figs. 3 and 4. In Figs. 1 and 3, the part of the components in the unit

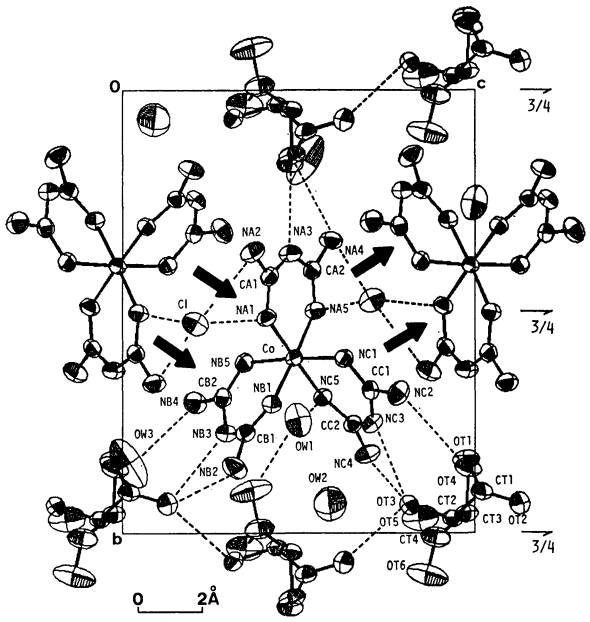


Fig. 1. An ORTEP drawing of the part of the components in the unit cell viewed down the a-axis with the numbering scheme for $(+)_{589}$-[Co(Hbg)$_3$]Cl(*d*-tart)·3H$_2$O. All atoms are drawn with 50% probability ellipsoids. Possible hydrogen bonds are indicated by broken lines. Hydrogen atoms are omitted for clarity.

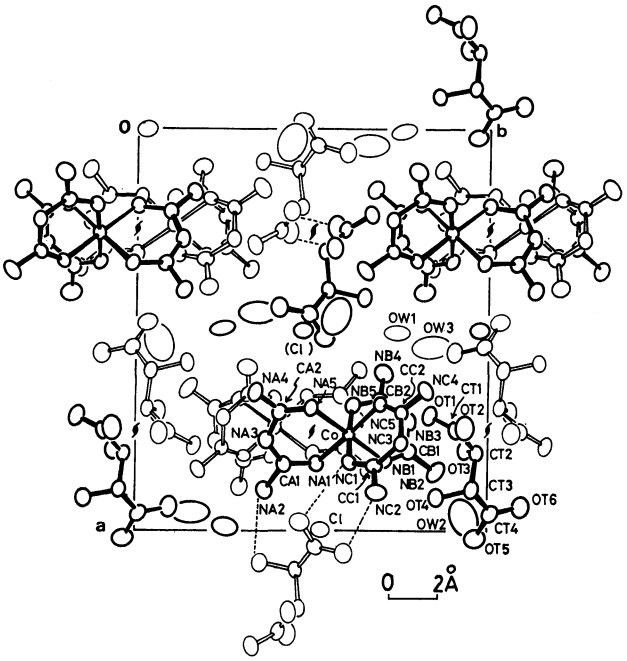


Fig. 2. An ORTEP drawing of the crystal structure viewed down the c-axis for $(+)_{589}$-[Co(Hbg)$_3$]Cl(*d*-tart)·3H$_2$O.

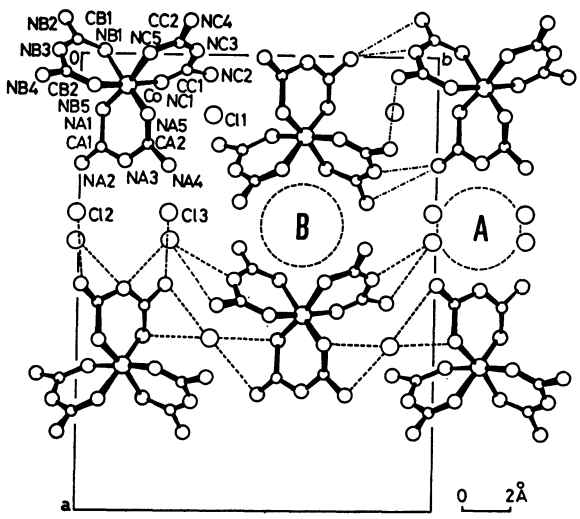


Fig. 3. A drawing of the part of the components in the unit cell projected on the (110) plane with the numbering scheme for $[Co(Hbg)_3]Cl_3$. Possible hydrogen bonds are indicated by broken lines. Hydrogen atoms are omitted for clarity. A and B indicate positions of void A and void B respectively.

cell are omitted in order to show the crystal features more clearly.

*Geometry of Complex Cation.* The bond distances and angles for the complex cation of both salts **1** and **2** are listed in Tables 4 and 5 respectively. They are in good agreement with those found in the two crystal structures, the less-soluble diastereomeric salt **3**, $(-)_{589}$-$[Co(Hbg)_3]Cl(d\text{-tart})\cdot 5H_2O$,[1] and the optically active chloride salt **4**, $(+)_{589}$-$[Co(Hbg)_3]Cl_3\cdot H_2O$:[2] averaged bond distances all differ by less than 0.012 Å and all averaged bond angles differ by less than 1.9°.

However, there is a small but significant difference in the geometry of complex cations among the four salts, **1**, **2**, **3**, and **4**. While the planarity of a biguanide ligand itself is bearly preserved in all these crystals, the planarity of a chelate ring as a whole (including the Co atom) is lost in some cases. The values of the dihedral angle between the plane of the Hbg ligand and the plane formed by Co and two donor N atoms are summarized in Table 6. The chelate ring A is approximately planar in all these crystals. In these crystals, two $Cl^-$ ions approach the chelate ring A from both sides. Deviation from the planarity is found for the chelate rings B and C in the diastereomeric salts **1** and **3**. In **1** and **3**, both chelate rings B and C are bent inside toward each other. This is clearly reflected by the shorter distances between the central imino-nitrogen atoms of the two chelate rings B and C (Table 6). It is not reasonable to assume the attraction between these two N atoms. The bending of the chelate ring plane being observed only in the crystals containing the *d*-tart anion, such a bending can be attributed to the electrostatic attraction by the *d*-tart anion.

*Geometry of* d-*Tart.* The bond distances and angles for the *d*-tart anion of the more-soluble salt **1** are listed in Table 4. These values are in accordance with those reported previously.[1,7,12] Five non-hydrogen atoms of each α-hydroxy carboxylate moiety lie approximately on a plane. The dihedral angle between the planes of the two moieties in the more-soluble salt **1** is 62.1°. This value is larger than the corresponding value of 50.8° in the less-soluble salt **3**. Such a relation in the dihedral angle has been found also in the crystal structures of two diastereomeric salt pairs containing the *d*-tartH anion $(C_4H_5O_6^-)$.[13-15]

*Crystal Packing.* *The More-soluble Salt* ***1***: The intermolecular distances and angles are summarized in Table 7. The complex cation and the $Cl^-$ ion are arranged alternately to form an infinite spiral chain, $\{\Delta\text{-}[Co(Hbg)_3]Cl\}_\infty$, along the twofold screw axis which is parallel to the c-axis through the position $(x=3/4, y=1/2)$ (Figs. 1 and 2). Hydrogen bonds are formed between the N atoms of Hbg A and the $Cl^-$ ion.

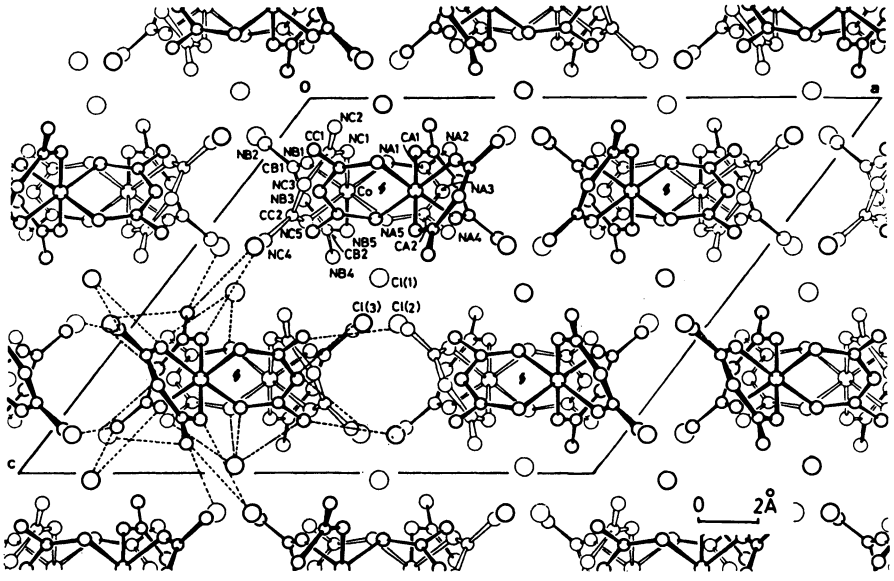


Fig. 4. A drawing of the crystal structure viewed down the b-axis for $[Co(Hbg)_3]Cl_3$. Possible hydrogen bonds are indicated by broken lines.

TABLE 4. BOND DISTANCES AND ANGLES (e.s.d.'s IN PARENTHESES) FOR $(+)_{589}$-$[Co(Hbg)_3]Cl \cdot d\text{-tart} \cdot 3H_2O$

| | | | | | | | |
|---|---|---|---|---|---|---|---|
| Bond distances $l$/Å | | | | | | | |
| Co–N(A1) | 1.921(3) | N(B5)–C(B2) | 1.292(5) | C(C2)–N(C3) | 1.371(5) | CT2–CT3 | 1.524(6) |
| Co–N(A5) | 1.925(3) | N(C1)–C(C1) | 1.287(5) | C(A1)–N(A2) | 1.370(5) | CT3–CT4 | 1.532(7) |
| Co–N(B1) | 1.907(3) | N(C5)–C(C2) | 1.301(5) | C(A2)–N(A4) | 1.341(5) | CT1–OT1 | 1.256(5) |
| Co–N(B5) | 1.933(3) | C(A1)–N(A3) | 1.361(5) | C(B1)–N(B2) | 1.365(6) | CT1–OT2 | 1.248(5) |
| Co–N(C1) | 1.919(3) | C(A2)–N(A3) | 1.381(5) | C(B2)–N(B4) | 1.349(5) | CT4–OT5 | 1.228(8) |
| Co–N(C5) | 1.904(3) | C(B1)–N(B3) | 1.376(5) | C(C1)–N(C2) | 1.347(5) | CT4–OT6 | 1 233(8) |
| N(A1)–C(A1) | 1.285(5) | C(B2)–N(B3) | 1.380(5) | C(C2)–N(C4) | 1.344(5) | CT2–OT3 | 1.427(5) |
| N(A5)–C(A2) | 1.281(5) | C(C1)–N(C3) | 1.381(5) | CT1–CT2 | 1.529(5) | CT3–OT4 | 1.436(6) |
| N(B1)–C(B1) | 1.280(5) | | | | | | |
| Bond angles $\phi$/° | | | | | | | |
| N(A1)–Co–N(A5) | 89.1(1) | N(C5)–C(C2)–N(C4) | 123.2(4) | N(C2)–C(C1)–N(C3) | 114 2(3) | | |
| N(B1)–Co–N(B5) | 88.4(1) | N(A1)–C(A1)–N(A3) | 122.6(4) | N(C4)–C(C2)–N(C3) | 115.1(3) | | |
| N(C1)–Co–N(C5) | 88.7(1) | N(A5)–C(A2)–N(A3) | 121.7(3) | OT1–CT1–OT2 | 125.3(4) | | |
| Co–N(A1)–C(A1) | 129.4(3) | N(B1)–C(B1)–N(B3) | 122.4(4) | OT1–CT1–CT2 | 117.9(4) | | |
| Co–N(A5)–C(A2) | 130.0(3) | N(B5)–C(B2)–N(B3) | 122.3(4) | OT2–CT1–CT2 | 116 8(4) | | |
| Co–N(B1)–C(B1) | 127.6(3) | N(C1)–C(C1)–N(C3) | 122.3(3) | CT1–CT2–OT3 | 110.1(3) | | |
| Co–N(B5)–C(B2) | 125.5(3) | N(C5)–C(C2)–N(C3) | 121.7(3) | CT1–CT2–CT3 | 109 8(3) | | |
| Co–N(C1)–C(C1) | 125.9(3) | C(A1)–N(A3)–C(A2) | 126.8(3) | OT3–CT2–CT3 | 110.0(3) | | |
| Co–N(C5)–C(C2) | 127.3(3) | C(B1)–N(B3)–C(B2) | 124.2(3) | CT2–CT3–OT4 | 107.9(3) | | |
| N(A1)–C(A1)–N(A2) | 122.1(4) | C(C1)–N(C3)–C(C2) | 125.0(3) | OT4–CT3–CT4 | 111.2(4) | | |
| N(A5)–C(A2)–N(A4) | 124.0(4) | N(A2)–C(A1)–N(A3) | 115.3(3) | CT2–CT3–CT4 | 110 2(4) | | |
| N(B1)–C(B1)–N(B2) | 124.0(4) | N(A4)–C(A2)–N(A3) | 114.2(3) | CT3–CT4–OT5 | 119.0(5) | | |
| N(B5)–C(B2)–N(B4) | 123.7(4) | N(B2)–C(B1)–N(B3) | 113.6(4) | CT3–CT4–OT6 | 117.4(5) | | |
| N(C1)–C(C1)–N(C2) | 123.4(4) | N(B4)–C(B2)–N(B3) | 114.0(3) | OT5–CT4–OT6 | 123.6(6) | | |

TABLE 5. BOND DISTANCES AND ANGLES (e.s.d.'s IN PARENTHESES) FOR $[Co(Hbg)_3]Cl_3$

| | | | | | | | |
|---|---|---|---|---|---|---|---|
| Bond distances $l$/Å | | | | | | | |
| Co–N(A1) | 1.907(6) | N(A1)–C(A1) | 1.279(11) | C(A1)–N(A3) | 1.366(14) | C(A1)–N(A2) | 1.348(12) |
| Co–N(A5) | 1.912(6) | N(A5)–C(A2) | 1.290(10) | C(A2)–N(A3) | 1.368(13) | C(A2)–N(A4) | 1.334(12) |
| Co–N(B1) | 1.896(6) | N(B1)–C(B1) | 1.292(10) | C(B1)–N(B3) | 1.386(11) | C(B1)–N(B2) | 1.336(12) |
| Co–N(B5) | 1.917(6) | N(B5)–C(B2) | 1.285(10) | C(B2)–N(B3) | 1.373(11) | C(B2)–N(B4) | 1.342(11) |
| Co–N(C1) | 1.922(6) | N(C1)–C(C1) | 1.281(10) | C(C1)–N(C3) | 1.369(11) | C(C1)–N(C2) | 1.351(12) |
| Co–N(C2) | 1.912(6) | N(C5)–C(C2) | 1.371(12) | C(C2)–N(C3) | 1.371(12) | C(C2)–N(C4) | 1.352(13) |
| Bond angles $\phi$/° | | | | | | | |
| N(A1)–Co–N(A5) | 89.6(3) | N(A5)–C(A2)–N(A4) | 123.4(8) | N(C5)–C(C2)–N(C3) | 122.0(8) | | |
| N(B1)–Co–N(B5) | 89.6(3) | N(B1)–C(B1)–N(B2) | 124.7(8) | C(A1)–N(A3)–C(A2) | 127.4(9) | | |
| N(C1)–Co–N(C5) | 89.5(3) | N(B5)–C(B2)–N(B4) | 124.5(7) | C(B1)–N(B3)–C(B2) | 126.8(7) | | |
| Co–N(A1)–C(A1) | 129.5(6) | N(C1)–C(C1)–N(C2) | 125.0(8) | C(C1)–N(C3)–C(C2) | 126.7(8) | | |
| Co–N(A5)–C(A2) | 129.6(6) | N(C5)–C(C2)–N(C4) | 122.4(8) | N(A2)–C(A1)–N(A3) | 114.4(8) | | |
| Co–N(B1)–C(B1) | 130.9(6) | N(A1)–C(A1)–N(A3) | 121.7(8) | N(A4)–C(A2)–N(A3) | 115.7(8) | | |
| Co–N(B5)–C(B2) | 128.9(5) | N(A5)–C(A2)–N(A3) | 120.9(8) | N(B2)–C(B1)–N(B3) | 114.9(8) | | |
| Co–N(C1)–C(C1) | 129.1(6) | N(B1)–C(B1)–N(B3) | 120.4(7) | N(B4)–C(B2)–N(B3) | 113.1(7) | | |
| Co–N(C5)–C(C2) | 129.5(6) | N(B5)–C(B2)–N(B3) | 122.4(7) | N(C2)–C(C1)–N(C3) | 112.7(7) | | |
| N(A1)–C(A1)–N(A2) | 123.9(8) | N(C1)–C(Cl)–N(C3) | 122.3(7) | N(C4)–C(C2)–N(C3) | 115.5(8) | | |

TABLE 6. DIHEDRAL ANGLES BETWEEN PLANE OF Hbg LIGAND AND PLANE FORMED BY Co AND TWO DONOR N ATOMS, AND DISTANCES BETWEEN CENTRAL IMINO N ATOMS

| | Chelate ring $\phi$/° | | | N(X3)···N(Y3) $l$/Å | | |
|---|---|---|---|---|---|---|
| | A | B | C | X=A, Y=B | X=A, Y=C | X=B, Y=C |
| 1 | 5.6 | 19.9 | 19.3 | 5.98 | 5.88 | 4.67 |
| 3 | 3.0 | 16.4 | 16.4 | 5.87 | 5.87 | 4.84 |
| 4 | 6.9 | 6.0 | 12.8 | 5.60 | 5.19 | 5.89 |
| 2 | 6.3 | 6.7 | 6.7 | 5.51 | 5.50 | 5.81 |

1: More-soluble salt. 2: Racemic salt. 3: Less-soluble salt. 4: Optically active salt.

If we assume a spiral chain which connects the complex and the Cl ions alternately along the hydrogen bonds as shown by broken lines in Fig. 1, the spiral arrangement is left-handed. However, the same spiral arrangement is considered to be right-handed, if we imagine a spiral chain which connects the central Co and Cl ions alternately as shown by arrows in Fig. 1. In this paper we take the latter definition. Such a spiral arrangement has been found in the crystal structures of **3** and **4**, too.[1] It is worth noting that the spiral configuration, $\{\Delta\text{-}[Co(Hbg)_3]Cl\}_\infty$, in **4** is right-handed, while that, $\{\Lambda\text{-}[Co(Hbg)_3]Cl\}_\infty$, in **3** is left-handed.

The *d*-tart anions are arranged along the c-axis to

Table 7. Selected intermolecular distances and angles for $(+)_{589}$-$[Co(Hbg)_3]Cl(d\text{-tart})\cdot 3H_2O$

| D–H···A | D···A $l$/Å | H···A $l$/Å | D–H···A $\phi$/° |
|---|---|---|---|
| N(A1)–H(NA1)···Cl | 3.415(3) | 2.50(4) | 156(3) |
| N(A2)–H(NA22)···Cl | 3.233(4) | 2.31(5) | 153(4) |
| N(A2)···OT4$^{i}$ | 3.291(5) | — | — |
| N(A3)–H(NA3)···OT1$^{ii}$ | 2.803(5) | 2 01(6) | 170(6) |
| N(A4)–H(NA41)···OT4$^{ii}$ | 3.141(5) | 2.47(5) | 141(5) |
| N(A4)$^{ii}$–H(NA42)···Cl | 3.305(4) | 2.47(6) | 163(5) |
| N(A5)$^{ii}$–H(NA5)···Cl | 3.495(3) | 2.73(6) | 154(4) |
| N(B1)$^{iii}$–H(NB1)···OW1 | 3.009(6) | 2.19(6) | 164(6) |
| N(B2)–H(NB21)···OT2$^{iv}$ | 2.936(6) | 2.15(6) | 150(5) |
| N(B2)$^{v}$–H(NB22)···Cl | 3.325(5) | 2.83(5) | 118(4) |
| N(B3)–H(NB3)···OT2$^{iv}$ | 2.863(5) | 2.04(5) | 151(4) |
| N(B3)···OT6$^{vi}$ | 3.275(7) | — | — |
| N(B4)–H(NB41)···OT5$^{iii}$ | 2.775(6) | 1.87(5) | 176(5) |
| N(B4)–H(NB42)···OW3 | 2.978(8) | 2.30(6) | 154(6) |
| N(C1)–H(NC1)···OT5$^{i}$ | 3.023(6) | 2.13(4) | 161(4) |
| N(C2)–H(NC21)···OT6$^{i}$ | 3.122(7) | 2.34(6) | 146(5) |
| N(C2)–H(NC22)···OT4 | 3.210(5) | 2.43(5) | 172(5) |
| N(C2)$^{iii}$···OW3 | 3.094(8) | — | — |
| N(C3)–H(NC3)···OT3 | 2.794(5) | 1.92(4) | 158(4) |
| N(C4)–H(NC41)···OT3 | 3.082(5) | 2.38(6) | 147(6) |
| N(C4)–H(NC42)···Cl$^{iii}$ | 3.338(4) | 2.54(8) | 121(5) |
| N(C4)···OT1 | 3.227(5) | — | — |
| N(C5)–H(NC5)···OW1 | 2.985(6) | 2.06(5) | 159(4) |
| OT3–H(OT3)···OT2$^{vi}$ | 2.792(5) | 1.93(5) | 162(5) |
| OW1–H(OW11)···OT6$^{vi}$ | 2.758(8) | 1.94(7) | 152(6) |
| OW1–H(OW12)···OW2$^{iii}$ | 2.712(9) | 1.83(6) | 175(6) |
| OW2$^{vi}$–H(OW21)···OW3 | 3.181(10) | 2.23(7) | 152(6) |
| OW2···OT5 | 2.969(9) | — | — |
| OW3–H(OW32)···OT4$^{iii}$ | 3.327(8) | 1.97(11) | 167(7) |
| OW3–H(OW31)···OT1$^{iv}$ | 2.693(8) | 1.55(7) | 167(6) |

Roman numerals as superscripts refer to the following equivalent positions relative to the reference molecule at $x, y, z$:

i ( $2-x, -1/2+y, 3/2-z$), ii ($3/2-x, 1-y, -1/2+z$), iii($-1/2+x, 3/2-y, 1-z$), iv( $x, y, -1+z$), v ( $2-x, -1/2+y, 1/2-z$), vi($3/2-x, 2-y, -1/2+z$)

D, hydrogen donor; A, hydrogen acceptor.

Table 8. Selected intermolecular distances and angles for $[Co(Hbg)_3]Cl_3$

| D–H···A | D···A $l$/Å | H···A $l$/Å | D–H···A $\phi$/° |
|---|---|---|---|
| N(A1)–H(NA1)···Cl(1)$^{i}$ | 3.401(6) | 2.49(8) | 159(7) |
| N(A2)–H(NA21)···Cl(2)$^{ii}$ | 3.218(9) | 2.33(10) | 152(9) |
| N(A2)–H(NA22)···Cl(1)$^{i}$ | 3.358(9) | 2.60(10) | 161(9) |
| N(A3)–H(NA3)···Cl(2)$^{iii}$ | 3.487(11) | 2.94(13) | 129(11) |
| N(A3)–H(NA3)···Cl(3)$^{iv}$ | 3.477(11) | 3.17(13) | 107(10) |
| N(A4)–H(NA41)···Cl(3)$^{v}$ | 3.233(9) | 2.45(9) | 162(8) |
| N(A4)–H(NA42)···Cl(1) | 3.333(9) | 2.48(14) | 149(11) |
| N(A5)–H(NA5)···Cl(1) | 3.387(7) | 2.52(11) | 151(9) |
| N(B1)–H(NB1)···Cl(1)$^{vi}$ | 3.497(6) | 2.73(9) | 154(8) |
| N(B2)–H(NB21)···Cl(1)$^{vi}$ | 3.330(9) | 2.59(10) | 151(9) |
| N(B2)–H(NB22)···Cl(3)$^{vi}$ | 3.233(9) | 2.31(11) | 157(9) |
| N(B3)–H(NB3)···Cl(3)$^{vii}$ | 3.457(8) | 2.74(12) | 144(10) |
| N(B4)–H(NB41)···Cl(3)$^{vii}$ | 3.307(8) | 2.59(10) | 146(9) |
| N(B4)–H(NB42)···Cl(2) | 3.621(8) | 2.79(11) | 164(9) |
| N(B5)–H(NB5)···Cl(2) | 3.629(7) | 2.75(10) | 149(8) |
| N(C1)–H(NC1)···Cl(3)$^{i}$ | 3.631(7) | 2.81(9) | 155(7) |
| N(C2)–H(NC21)···Cl(2)$^{vi}$ | 3.296(9) | 2.52(15) | 151(13) |
| N(C2)–H(NC22)···Cl(2)$^{ix}$ | 3.290(9) | 2.70(12) | 133(10) |
| N(C2)–H(NC22)···Cl(3)$^{i}$ | 3.631(7) | 3.04(12) | 135(9) |
| N(C3)–H(NC3)···Cl(2)$^{vi}$ | 3.463(9) | 2.67(10) | 146(8) |
| N(C4)–H(NC41)···Cl(1)$^{vii}$ | 3.316(11) | 2.58(10) | 141(8) |
| N(C4)–H(NC42)···Cl(2)$^{vii}$ | 3.234(11) | 2.30(10) | 156(8) |
| N(C5)–H(NC5)···Cl(1)$^{vii}$ | 3.482(6) | 2.72(10) | 151(9) |

Roman numerals as superscripts refer to the following equivalent positions relative to the reference molecule at $x, y, z$:

i ( $1/2-x, -1/2+y, 1/2-z$),
ii ( $x, -y, -1/2+z$),
iii ( $1-x, -y, 1-z$),
iv ( $x, 1-y, -1/2+z$),
v ( $1-x, 1-y, 1-z$),
vi ($-1/2+x, 1/2-y, -1/2+z$),
vii( $1/2-x, 1/2-y, 1-z$),
viii( $x, -1+y, z$),
ix ( $1/2-x, 1/2+y, 1/2-z$),
x ( $1-x, y, 3/2-z$)

D, hydrogen donor; A, hydrogen acceptor.

make an infinite chain, $(d\text{-tart})_\infty$, in which two adjacent anions are related by the twofold screw axis (Figs. 1 and 2). A hydrogen bond is formed between the O atoms of hydroxyl and carboxylato groups of adjacent *d*-tart anions, OT3–H(OT3)···OT2$^{vi}$ 2.792 Å. The pitch of the chain is equal to the length of the c-axis, 11.010 Å. A similar infinite chain related by the twofold screw axis has been found in several crystals containing the *d*-tart anions.[16-20] In these crystals the pitch of the chain shows a wide variation from 6.128 Å in $(NH_4)_2\cdot d\text{-tart}$[18] to 10.989 Å in $[Pt(en)_2]d\text{-tart}$.[20] The pitch in the present case (11.010 Å) is the longest one ever observed. The framework of the crystal structure is built up of two kinds of chains, $\{\Delta\text{-}[Co(Hbg)_3]Cl\}_\infty$ and $(d\text{-tart})_\infty$, along the c-axis. These chains are closely packed with each other (Fig. 2).

As shown in Table 1, the $V/Z$ value, 592.8 Å$^3$, of **1** is 103.7 Å$^3$ smaller than that, 696.5 Å$^3$, of **3**. When the volume ($2\times 20.6$ Å$^3$)[21] corresponding to two water molecules (the difference in the number of water of crystallization between **1** and **3**) is subtracted from the $V/Z$ value of **3**, a large positive value, 62.5 Å$^3$, still remains. Thus, it can be concluded that the packing density in the more-soluble salt **1** is larger than that in the less-soluble salt **3**. This makes a marked contrast to the cases of two diastereomeric salt pairs containing *d*-tartH, in which the packing density is larger in the less-soluble salt than in the more-soluble salt.[13-15]

*The Racemic Chloride Salt* **2**: The intermolecular distances and angles are summarized in Table 8. The complex cation of the same chirality and a kind of $Cl^-$ ions (Cl(1)) are arranged alternately along the twofold screw axis to form an infinite spiral chain, $\{[Co(Hbg)_3]Cl\}_\infty$, which is similar to that found in the crystal structures, **1**, **3**, and **4**, (Figs. 3 and 4). Moreover, the spiral chain made up of the *Λ* complex is left-handed and that made up of the *Δ* complex is right-handed. Short contacts between some N atoms of adjacent complexes are 3.21(1)—3.43(1) Å (Fig. 3). The distances between H and N atoms are H(NB22)···N(A4)

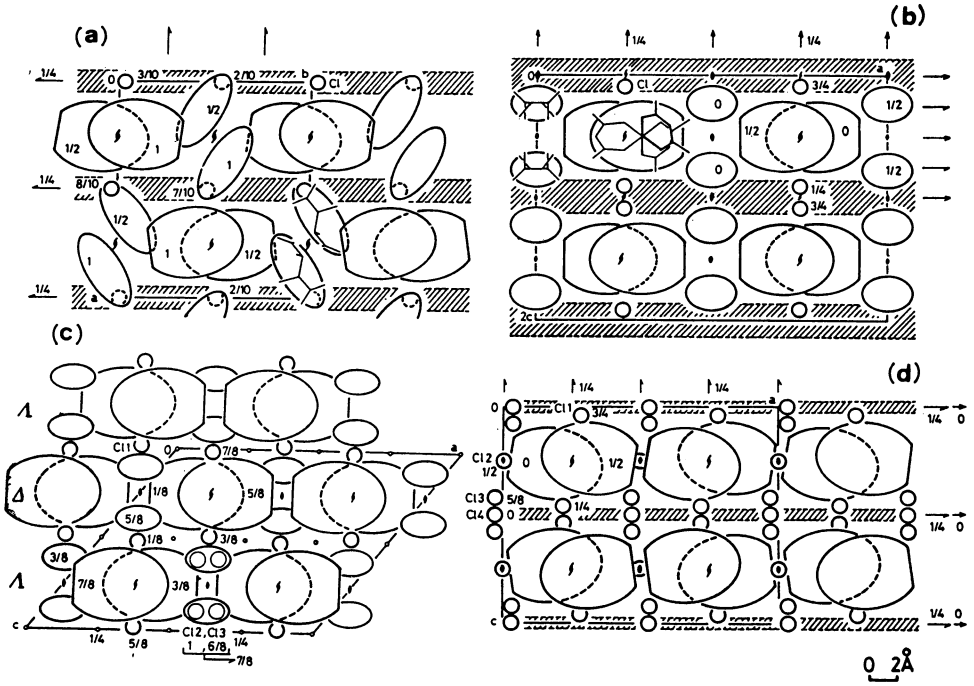


Fig. 5. A schematic drawing of the crystal structures of the four salts, (a) the more-soluble salt $(+)_{589}$-$[Co(Hbg)_3]Cl(d\text{-tart})\cdot 3H_2O$ **1**, (b) the less-soluble salt $(-)_{589}$-$[Co(Hbg)_3]Cl(d\text{-tart})\cdot 5H_2O$ **3**, (c) the racemic salt $[Co(Hbg)_3]Cl_3$ **2**, and (d) the optically active salt $(+)_{589}$-$[Co(Hbg)_3]Cl_3\cdot H_2O$ **4**, along the c-axis for **1** and the b-axis for **2**, **3**, and **4**. Shaded parts indicate positions of water molecules.

2.85(11), H(NB3)···N(A4) 2.63(12), H(NB42)···N(C2) 2.83(11), and H(NC3)···N(A2) 2.65(10) Å. These values are close to the sum, 2.75 Å, of van der Waals radii of H, 1.20 Å, and N, 1.55 Å, atoms.[22] Therefore, the complex cations tend to pack together as closely as their geometry allows in the formation of the spiral chains.

*Comparison of the Packing Modes of the Four Salts, **1**, **2**, **3**, and **4**.* The most characteristic point common to all these four crystal structures is that they contain the infinite spiral chain, $\{[Co(Hbg)_3]Cl\}_\infty$. The four crystal structures projected along the infinite spiral chain are shown schematically in Fig. 5. In these crystals, the spiral chains are packed in parallel with each other.

In the racemic salt **2** and the optically active salt **4**, the spiral chains are arranged almost in contact with each other, and the remaining two $Cl^-$ ions are placed in a void formed by the arrangement of the spiral chains. Here, if we regard the spiral chain as a cylinder, the packing mode in **2** and **4** can be regarded as somewhat irregular, hexagonal and tetragonal packings of parallel cylinders respectively. These two modes, hexagonal and tetragonal, are known as two types of the simplest packings of parallel cylinders. Moreover, the density of the hexagonal packing is larger than that of the tetragonal packing.[23] Indeed, the density of **2** is larger than that of **4** (Table 1).

In the racemic salt **2**, the spiral chains of the same chirality are related along the a-axis by the twofold operation to form a chiral layer on the ab plane as shown in Figs. 4 and 5(c). Also in the less-soluble salt **3** and the optically active salt **4**, the spiral chains are related along the a-axis by the same twofold operation (Figs. 5(b) and 5(d)). Therefore, in these crystals, the voids formed between the adjacent spiral chains on the ab plane can be divided roughly into two groups; one is between two Hbg A (void A) and the other is between Hbg B and C (void B) (see Fig. 3). In **2**, two kinds of $Cl^-$ ions (Cl(2) and Cl(3)) are concentrated in void A to form $(4^-)$-charged conglomerate. The distances between these $Cl^-$ ions are Cl(2)···Cl(2)$^x$ 3.907(4), Cl(3)···Cl(3)$^x$ 3.908(4), and Cl(2)···Cl(3) 4.106(4) Å. These distances seem to be fairly short, considering the radius of the $Cl^-$ ion of 1.81 Å.[24] In **3**, it has been found that two *d*-tart anions are concentrated in voild A to form a dimeric unit, $(d\text{-tart})_2^{4-}$ (Fig. 5(b)). Therefore, the packing mode in the layer for **2** bears a striking resemblance to that in the layer for **3**. In **4**, three kinds of $Cl^-$ ions (Cl(2), Cl(3), and Cl(4)) are not concentrated in a particular void but scattered in the whole crystal (Fig. 5(d)).

On the other hand, in the more-soluble salt **1**, the spiral chains are related along the b-axis by a unit translation and the relation of the adjacent spiral chains in **1** is different from that in the other three crystals, **2**, **3**, and **4** (Fig. 5(a)). Therefore, in **1**, Hbg A always faces with Hbg B and C in the adjacent spiral chains along the b-axis. The *d*-tart anions are evenly distributed in the void formed by the arrangement of the spiral chains. As a result, the *d*-tart anions themselves form an infinite chain, $(d\text{-tart})_\infty$, through hydrogen bonds (–OH···OOC–). Thus, the packing mode of **1** resembles that of **4** in terms of a dispersive distribution

of the counter anions. Therefore, it might be assumed that the localization of negative charges plays a dominant role in the stabilization of the crystal structure for the less-soluble salt **3** and the racemic salt **2**.

*Chiral Discrimination Mode.* Since the complex ions, $\Delta$ and $\Lambda$, in these four crystals are linked together *via* $Cl^-$ ions to form the infinite spiral chains, {$\Delta$-[Co(Hbg)$_3$]Cl}$_\infty$ and {$\Lambda$-[Co(Hbg)$_3$]Cl}$_\infty$, we can safely conclude that the chiral discrimination by the *d*-tart anion is effected not on the individual complex ion but on these infinite chains in the diastereomer formation. Namely, the crystal-packing mode as a whole is responsible for the chiral discrimination. Here, the question is how the *d*-tart anions collect the spiral chains of the same chirality to form a crystal.

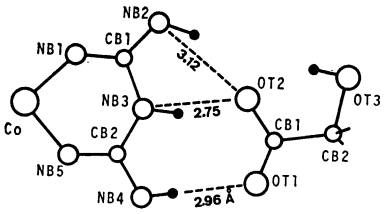


Fig. 6. Disposition of the Hbg ligand and the α-hydroxy carboxylate moiety of the *d*-tart anion for the less-soluble salt **3**. The broken lines indicate hydrogen bonds.

In relation to this point, in the less-soluble salt **3**, a specific close contact between Hbg B (Hbg C is equivalent to Hbg B in crystallography) and *d*-tart has been found along the twofold axis of complex. This specific close contact between the guanidino moiety of Hbg and carboxylato group of *d*-tart is illustrated in Fig. 6. The atoms in Hbg and α-hydroxy carboxylate moiety of *d*-tart lie on nearly the same plane. In the previous paper,[1] it was presumed that this specific close contact (specific interaction) plays a dominant role in collecting left-handed spiral chains. This specific close contact mode is expected to be more stable than any other modes of interaction between the guanidino moiety and the carboxylato group.[25] In other words, it is concluded that this specific close contact mode is most reasonable mode of access for the *d*-tart anion to combine the left-handed spiral chains. It is worth noting that a similar specific interaction has been found between the guanidyl group of arginine and the γ-carboxylato group of glutamate in the crystal structure of L-arginine L-glutamate.[26]

Such a specific close contact mode is not found in the more-soluble salt **1**. A complex cation is surrounded by six *d*-tart anions through hydrogen bonds in different modes of close contact, among which the mode of access to the complex nearly along the threefold axis seems to be important in relation to chiral discrimination as shown in Figs. 2 and 7. One α-hydroxy carboxylate moiety of *d*-tart are hydrogen-bonded to the adjacent *d*-tart anions related by the twofold screw axis to form an infinite chain, (*d*-tart)$_\infty$, as shown by a broken line A in Fig. 7. On both sides of this infinite chain, are running parallel two infinite spiral chains, {$\Delta$-[Co(Hbg)$_3$]Cl}$_\infty$. The other α-hydroxy carboxylate moiety

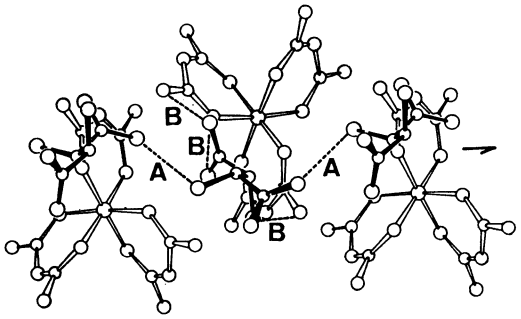


Fig. 7. Disposition of the *d*-tart anions in (*d*-tart)$^\infty$ and the complex cations in {$\Delta$-[Co(Hbg)$_3$]Cl}$_\infty$ for the more-soluble salt **1**. Broken lines A and B indicate OH···O and NH···O hydrogen bonds respectively.

of each *d*-tart is hydrogen-bonded to Hbg A and C of each complex in these two infinite chains, {$\Delta$-[Co(Hbg)$_3$]Cl}$_\infty$, as shown by a broken line B in Fig. 7. Through such hydrogen bonds, the right-handed, spiral chains are collected by the infinite chain, (*d*-tart)$_\infty$. This is supported by the pitch of the two infinite chains (11.010 Å). Namely, in the spiral chain {[Co(Hbg)$_3$]Cl}$_\infty$, the pitch is considerably short when it is compared with pitches of other spiral chains, 12.970, 14.086, and 14.901 Å in **3**, **4**, and **2** respectively (Table 1), and in the chain, (*d*-tart)$_\infty$, the pitch is long when it is compared with pitches of other chains, (*d*-tart)$_\infty$, found so far.[16–20]

Therefore, it is clear that the more-soluble salt **1** is quite different from the less-soluble salt **3** in the close contact mode between the complex and *d*-tart ions. Here, the question is why the salt **3** is less-soluble than the salt **1**. Previously, in the crystal structures of two diastereomeric salt pairs containing *d*-tartH, it has been found that the density of the less-soluble salt is larger than that of the more-soluble salt, and the cation and the anion in the less-soluble salt fit with each other more compactly than those in the more-soluble salt (compact fitting model).[13–15] Contrary to the *d*-tartH systems, in the present case the density of the less-soluble salt **3** is smaller than that of the more-soluble salt **1**. In the present diastereomeric salt pair, no significant difference is found in the number of the hydrogen bonds and in the distances between the cation and the anion. Thus, the compact fitting model can not be applied successfully to the present diastereomeric salts. This seems to be due to quite different arrangements of *d*-tart: the infinite chain, (*d*-tart)$_\infty$, for **1** and the dimeric unit, (*d*-tart)$_2^{4-}$, for **3**. From the comparison of the crystal structures of the four salts, **1**, **2**, **3**, and **4**, it should be considered that the difference in the arrangement of the *d*-tart anions is important for the solubility difference in the present case. It can be concluded that the localization of the negative charge, which results from the formation of the dimeric unit (*d*-tart)$_2^{4-}$ containing the specific interaction between Hbg and *d*-tart, plays a dominant role in the stabilization of the crystal structure for the less-soluble diastereomeric salt **3**.

We wish to acknowledge a Grant-in-Aid for Scientific Research from the Ministry of Education, Science and Culture.

**References**

1) T. Tada, Y. Kushi, and H. Yoneda, *Bull. Chem. Soc. Jpn.*, **54**, 1538 (1981).
2) M. R. Snow, *Acta Crystallogr., Sect. B*, **30**, 1850 (1974).
3) D. Karipides and W. C. Fernelius, *Inorg. Synth.*, Vol. VII, 56 (1963).
4) P. Ray and N. K. Dutt, *J. Indian Chem. Soc.*, **16**, 621 (1939).
5) P. Ray and N. K. Dutt, *J. Indian Chem. Soc.*, **18**, 289 (1941).
6) K. Igi, T. Yasui, J. Hidaka, and Y. Shimura, *Bull. Chem. Soc. Jpn.*, **44**, 426 (1971).
7) J. M. Bijvoet, A. F. Peerdeman, and A. J. van Bommel, *Nature*, **168**, 271 (1951).
8) "International Tables for X-Ray Crystallography," Kynoch Press, Birmingham (1974), Vol. IV, pp. 72—79, 149.
9) Y. Kushi, unpublished work.
10) T. Ashida, "The Universal Crystallographic Computation Program System," ed by T. Sakurai, The Crystallographic Society of Japan (1967).
11) C. K. Johnson, ORTEP, Report ORNL-3794, Oak Ridge National Laboratory, Oak Ridge, Tennessee, U. S. A., 1965.
12) For example, R. Sadanaga, *Acta Crystallogr.*, **3**, 416 (1950); S. Perez, *ibid., Sect. B*, **33**, 1083 (1977); D. H. Templeton, A. Zalkin, H. W. Ruben, and L. K. Templeton, *ibid.*, **35**, 1608 (1979); L. S. Magill, J. D. Korp, and I. Bernal, *Inorg. Chem.*, **20**, 1187 (1981).
13) M. Kuramoto, Y. Kushi, and H. Yoneda, *Bull. Chem. Soc. Jpn.*, **51**, 3251 (1978).
14) M. Kuramoto, *Bull. Chem. Soc. Jpn.*, **52**, 3702 (1979).
15) M. Kuramoto, Y. Kushi, and H. Yoneda, *Bull. Chem. Soc. Jpn.*, **53**, 125 (1980).
16) G. K. Ambady, *Acta Crystallogr., Sect. B*, **24**, 1548 (1968).
17) H. Hinazumi and T. Mitsui, *Acta Crystallogr., Sect. B*, **28**, 3299 (1972).
18) V. S. Yadava and V. M. Padmanabhan, *Acta Crystallogr., Sect. B*, **29**, 493 (1973).
19) S. Perez, *Acta Crystallogr., Sect. B*, **32**, 2064 (1976).
20) W. A. Freeman, *Inorg. Chem.*, **15**, 2235 (1976).
21) K. Harata, *Bull. Chem. Soc. Jpn.*, **49**, 2066 (1976).
22) A. Bondi, *J. Phy. Chem.*, **68**, 441 (1964).
23) M. O'Keeffe and S. Andersson, *Acta Crystallogr., Sect. A*, **33**, 914 (1977).
24) L. Pauling, "The Nature of The Chemical Bond," 3rd ed, Cornell University Press, Ithaca (1960), p. 260.
25) E. Friedem, *J. Chem. Educ.*, **52**, 754 (1975).
26) T. N. Bhat and M. Vijayan, *Acta Crystallogr., Sect. B*, **33**, 1754 (1977).